Focal hemodynamic responses in the stimulated hemisphere during high-definition transcranial direct current stimulation

Abstract

Objective: High-definition tDCS (HD-tDCS) using a 4x1 electrode montage has been previously shown to constrain the electric field within the spatial extent of the electrodes. The aim of this study was to determine if functional near-infrared spectroscopy (fNIRS) neuroimaging can be used to determine a hemodynamic correlate of this 4x1 HD-tDCS electric field on the brain.

Materials and Methods: In a 3 session cross-over study design, 13 healthy males received sham (2mA, 30s) and real (HD-tDCS-1 and HD-tDCS-2, 2mA, 10min) anodal HD-tDCS targeting the left M1 via a 4x1 electrode montage (anode C3, 4 return electrodes 3.5cm from anode). fNIRS was used to measure changes in brain hemodynamics (oxygenated hemoglobin integral-O_2Hb_{int}) during each 10min session from 2 regions of interest (ROIs) in the stimulated left hemisphere that corresponded to "within" (L_{in}) and "outside" (L_{out}) the spatial extent of the 4x1 electrode montage, and 2 corresponding ROIs (R_{in} and R_{out}) in the right hemisphere.

Results: The ANOVA showed that both real anodal HD-tDCS compared to sham induced a significantly greater O_2Hb_{int} in the L_{in} than L_{out} ROIs of the stimulated left hemisphere; while there were no significant differences between the real and sham sessions for the right hemisphere ROIs. Intra-class correlation coefficients for the 2 real HD-tDCS sessions showed "fair to good" reproducibility for L_{in} (0.54) and L_{out} (0.52) ROIs.

Conclusion: The greater O_2Hb_{int} "within" than "outside" the spatial extent of the 4x1 electrode montage represents a hemodynamic correlate of the electrical field distribution, and thus provides a prospective reliable method to determine the dose of stimulation that is necessary to optimize HD-tDCS parameters in various applications.

Keywords: tDCS, fNIRS, motor cortex stimulation, blood flow, electric field

Introduction

Transcranial direct current stimulation (tDCS) is a non-invasive and portable brain stimulation technology that has potential to positively augment the human brain to enhance a variety of cognitive/motor skills that should ultimately improve behavioural performance (1, 2). For the purpose of augmenting motor skills, anodal tDCS is usually applied to scalp overlying the primary motor cortex (M1) with a currently intensity of 1-2mA over 10-20min duration. Most research groups have used a conventional electrode montage of two large 35 cm^2 (7 x 5 cm^2) rectangular rubber-sponge electrodes with the anode electrode placed on the M1 and return electrode on the contralateral supraorbital region (3) or extracephalic region such as the shoulder (4). These tDCS parameters and montages are generally shown to increase M1 excitability and activity during and for a short period (min to hours) after anodal tDCS (5).

The mechanism(s) of anodal tDCS-induced neuromodulatory effects are related to subthreshold neuronal membrane depolarization directly induced by the tDCS electric field with subsequent increases in spontaneous neuronal firing rates coupled with synaptic neuroplasticity (5). However, the imprecise understanding of the specific neurophysiological changes induced by scalp-applied electric fields limits efforts to understand its precise mechanisms of action, as well as optimize stimulation protocols. Consequently, tDCS parameters and montage are commonly applied uniformly between subjects without consideration for anatomical and physiological differences between individuals, which may account in part to the variability in responses to tDCS that is recently being reported in the literature (6, 7). This is a growing concern among researchers as the number of tDCS studies increases and reproducibility concerns are a problem (8, 9).

In order to circumvent the limitations in directly measuring the tDCS electric field, studies have attempted to optimize tDCS applications using computational modeling of current flow between the electrodes in order to predict brain regions the tDCS current passes through

or directly engages. These modeling approaches have been applied to derive optimal electrode montages (10), as well as the design of multiple small electrode (~3cm^2) high-definition (HD) montages to focalize distribution of tDCS current to a target brain region (11). For example, in anodal HD-tDCS using a 4x1 electrode montage, the anode electrode is placed at the centre overlying the M1 with four return electrodes placed ~3.5cm away from the anode in a ring configuration (12, 13). Compared to conventional tDCS montages, the 4x1 HD-tDCS montage has been shown to constrain the electric field between the active electrode and four surrounding return electrodes, and thus focally stimulate a target cortical region (14), and potentially increase the long-lasting excitability after-effects (12). Although modeling approaches have been applied to derive optimal electrode montages and dosages for tDCS (10), the estimates of tDCS current distribution remain theoretical and await experimental validation. Therefore, in order to optimize 4x1 HD-tDCS montage potential applications to enhance motor and cognitive performance, there is a critical need to identify a neurophysiological correlate of the electric field spatial distribution from the scalp-applied current.

Neuroimaging methods can be used to provide information about the brain-tissue effects of the tDCS electric fields when measured in a resting-state during (15-22) and/or after (23-25) neurostimulation. Hemodynamic based neuroimaging methods, such as positron emission tomography (PET), functional magnetic resonance imaging (fMRI) and functional near-infrared spectroscopy (fNIRS), detect cerebral hemodynamic changes based on neurovascular coupling mechanisms (26, 27). Lang et al. (24) using PET and a conventional anodal tDCS montage (anode M1, cathode on opposite supraorbital region) showed increased regional cerebral blood flow (rCBF) under the stimulating electrodes, as well as widespread increases in rCBF in cortical and subcortical areas up to 50min after tDCS. Although rCBF measurements after tDCS provide information on the after-effects of tDCS, measuring rCBF during tDCS is the only way to determine the direct brain tissue effects of tDCS electrical fields. Zheng et al.,

(16) using fMRI-arterial spin labeling measurements during conventional anodal tDCS with interleaved 7min On/Off stimulation periods showed current intensity related increases in rCBF in brain regions under and in close proximity to the stimulating electrodes as well as a widespread network, specifically involving contralateral motor-related cortical areas. These localized increases in rCBF under the stimulating electrodes during anodal tDCS have also been demonstrated in the prefrontal cortex by Stagg et al. (15) using a similar fMRI method.

Since fMRI and PET neuroimaging methods are immobile, large, expensive, and require complicated analysis methods, they are not suitable for routine in-vivo visualization of tDCS induced effects on brain tissues in natural settings such as a clinic. Furthermore, due to the nature of fMRI measurements there are issues regarding the role tDCS-induced current flow itself producing an artifact or distortion of the fMRI signal considering that applied currents generate magnetic fields and these may interfere with the MRI imaging sequences which rely on carefully controlled magnetic field distributions (28). Furthermore, there are safety concerns of fMRI causing heating in wires and electrodes on the scalp of subjects that may not be properly insulated, and in the case of PET, there are concerns of radiation and invasiveness of the method to inject radiolabels (29).

fNIRS being a non-invasive and portable optical neuroimaging technique is ideal for in-vivo monitoring of brain hemodynamics during and/or after tDCS in naturalistic settings (4, 13, 20-22, 25, 30-33). Moreover, since fNIRS uses optically based measurements of light intensity, it is not influenced by electrically induced artifacts. fNIRS uses scalp based light emitting probes to measure the time course of changes in the concentrations of oxygenated (O_2Hb) and deoxygenated (HHb) hemoglobin in both extracranial (skin) and intracranial (cerebral) compartments of the brain (34). A previous multi-channel fNIRS study by Khan et al., (20) using a bi-hemispheric tDCS montage (anode M1, cathode on opposite M1) showed an increase and then plateau in O_2Hb under the anode electrode during the initial 3min of stimulation,

however, no specific description of the spatial distribution of O_2Hb relative to the stimulating electrodes was provided. Thus far, only our previous pilot study (21) utilized a 2-channel fNIRS setup (one channel on each hemisphere) to measure the time course of changes in O_2Hb during anodal HD-tDCS (2mA, 10min) using a 4x1 electrode montage targeting the left M1. We showed that O_2Hb increases in close proximity to the anode located on the left hemisphere with a steady rise over the initial stimulation period with peak levels attained within 2-5min of the onset of stimulation with these levels maintained at relative plateau throughout the remaining stimulation period. No consistent changes in O_2Hb were found in the right hemisphere measurement point. Since our previous study used one fNIRS channel on each hemisphere, we were not able to determine the spatial distribution of the time course of O_2Hb during 4x1 HD-tDCS.

Although portable and non-invasive electroencephalography approaches using scalp based electrodes can be used to determine neurophysiological correlates of electric field propagation within the brain during tDCS in natural settings (18, 19), this method faces the fundamental biophysical limits imposed by the scalp, skull and brain as volume conductors that limit spatial resolution, and the need to remove artefacts imposed by the tDCS-induced currents limits its application for in-vivo online monitoring. fNIRS provides a solution to this, since spatial locations of changes in hemodynamics are predicted between the boundaries of the transmitter-detector locations that are usually 3cm apart, such that changes in fNIRS parameters provide an accurate measurement of the spatial hemodynamic changes with a resolution of 2-3cm.

Therefore the aim of this study was to utilize multi-channel fNIRS neuroimaging to measure in-vivo changes in O_2Hb during anodal HD-tDCS (2mA, 10min) with a 4x1 electrode montage and thus provide a hemodynamic correlate of the spatial distribution of this HD-tDCS electric field. We hypothesized the 4x1 HD-tDCS electric field would 1) increase O_2Hb in the

regions within the spatial extent of the 4x1 electrode montage in the left stimulated hemisphere to a greater extent than regions outside this boundary, 2) the changes in O_2Hb in the corresponding regions of the right non-stimulated hemisphere would show no or minimal changes compared to the left side, 3) the changes in O_2Hb in the left hemisphere will be reproducible.

Materials and Methods

Subjects

Fifteen healthy males volunteered to participate in the study, however, two subjects had to be excluded due to missing a session or inadequate data for analysis. The remaining 13 Subjects (34.2 ± 12.3 years) were right handed (laterality quotient 82.8 ± 14, range from 58 to 100) as determined by the Edinburgh handedness questionnaire (Oldfield, 1971). The study conformed to the recommendations of the local Human Research Ethics Committee in accordance with the Declaration of Helsinki, and all participants gave written informed consent after a description of the study procedures and associated risks.

Design and Protocol

In a 3 session cross-over study design, subjects were randomly allocated to initially receive either sham or one of 2 identical real (HD-tDCS-1 or HD-tDCS-2) anodal HD-tDCS sessions targeting the left M1 via a 4x1 electrode montage with 1 week separating each session. The two real HD-tDCS sessions afforded a within-subject replication of the findings. In the 2 real HD-tDCS sessions, active stimulation was applied with 30s ramp up to 2mA and maintained at this level for 10min duration. In sham, active stimulation was applied with 30s ramp up to 2mA, 30s at 2mA, and 30s ramp down (total active stimulation: 1.5min) followed by no stimulation

for the remaining 8.5min. We undertook this type of active sham stimulation to provide the same sensations on the scalp as those of the real HD-tDCS sessions.

For each session, after the experimental setup, fNIRS measurements were initiated with 3min of baseline followed by the specific stimulation session, in which participants were asked to relax for the duration of the session. During each anodal HD-tDCS session, fNIRS was used to simultaneously measure changes in brain hemodynamics from 16 channels covering the scalp of the left (stimulated) and right (unstimulated) hemispheres.

HD-tDCS

A Startstim tDCS system (Neuroelectrics, Barcelona, Spain) was used to deliver constant direct currents to the left M1 via an anodal 4x1 HD-tDCS electrode montage (13). The active anode electrode was positioned on the scalp at C3 surrounded by four return electrodes each at a distance of ~3.5 cm from the anode electrode at FC1, FC5, CP5 and CP1 based on the 10-10 EEG system. The five HD-tDCS electrodes (3.14 cm^2 AgCl electrodes) were secured on the scalp using conductive paste (Ten20®, Weaver and Company, USA) and held in place using a specially designed plastic headgear to hold the HD-tDCS electrodes and fNIRS probes on the head (see Figure 1).

fNIRS

A continuous-wave fNIRS device (Oxymon MK III, Artinis Medical Systems, The Netherlands) was used to continuously measure changes in O_2Hb and HHb concentrations from 16 channels (Ch) covering the scalp of the left (Ch1-8) and right (Ch9-16) hemispheres with a 3 cm transmitter-detector distance (see Figure 1). A 3D-digitizer (Fastrack, Polhemus, United States) and MATLAB toolbox NFRI_function (Singh et al., 2005) was used to estimate the Montreal Neurological Institute coordinates (MNI) of the location of each fNIRS probe and

HD-tDCS electrode. Based on the anatomical locations of brain areas, we designated four regions of interests (ROIs): the two left hemisphere ROIs corresponded to "within" (L_{in}: Ch3,4,5,6) and "outside" (L_{out}: Ch1,2,7,8) the spatial extent of the 4x1 electrode montage (see Figure 1). For the right hemisphere, two spatially corresponding ROIs were also determined (R_{in}: Ch11,12,13,14 and R_{out}: Ch9,10,15,16).

Data analysis

All fNIRS data analysis was undertaken using Oxysoft V3.0.103 (Artinis Medical Systems, The Netherlands). The changes in O_2Hb and HHb concentrations (expressed in μM) were calculated according to a modified Beer-Lambert Law that included an age-dependent constant differential pathlength factor ($4.99+0.067*Age^{0.814}$) (35).

The time course of changes in O_2Hb and HHb concentrations for each of the 16 channels were first low-pass filtered at 0.1 Hz to attenuate cardiac signal, respiration, and Mayer-wave systemic oscillations (35), and then offset to zero at the start of each stimulation session. HHb time course did not show robust changes compared to O_2Hb over the 10min stimulation period, so we focused on O_2Hb. The O_2Hb integral (O_2Hb_{int}) value of each of the 16 channels of each subject was then calculated over a 600s period after stimulation onset. Since we found no significant difference between the anterior and posterior portions of the "outside" ROIs in the left (Ch1,2 and Ch7,8, respectively) and right (Ch9,10 and Ch15,16, respectively) hemispheres, we combined the two portions to represent L_{out} and R_{out} ROIs, respectively. Subsequently, the group average O_2Hb_{int} value was calculated for each ROI (L_{in}, L_{out}, R_{in}, R_{out}).

Statistics

SigmaPlot 12 (Systat Software Inc, CA, USA) software was used for statistical analysis. All data were first screened for normality of distribution and homogeneity of variance using a

Shapiro-Wilk and Levene's test, respectively. For statistical analysis of the O_2Hb integral (O_2Hb_{int}) values, a Session (HD-tDCS-1, HD-tDCS-2, sham) x ROI (L_{in}, L_{out}, R_{in}, R_{out}) repeated measures ANOVA was used. If a significant main or interaction effect was evident, then Bonferroni corrected post-hoc tests were performed. Intraclass correlation coefficients (ICC(2,1)) were calculated between the two real HD-tDCS sessions (HD-tDCS-1 and HD-tDCS-2) to test the repeatability of the O_2Hb_{int} results. Significance was set at $P \leq 0.05$. Data are presented as mean ± SD.

Results

Figure 2 shows a representative subjects' time course of O_2Hb changes in the left (a) and right (b) hemisphere ROIs during 10min of sham and real anodal HD-tDCS. For the real HD-tDCS session, the O_2Hb time course in the stimulated left hemisphere ROIs (L_{in}, L_{out}) showed, after an initial decrease, a steady increase from baseline over the first 3min of stimulation period with a relative plateau maintained for the duration of the stimulation period; however, the L_{in} ROI showed a faster rise and greater amplitude in the hemodynamic response than L_{out} ROI. During the sham session, O_2Hb in the left ROIs also increased after an initial slight dip during the 90s active stimulation period (30s ramp up from 0mA to 2mA, 30s at 2mA, and 30s ramp down to 0mA) and then gradually returned to baseline levels over the next 8.5min measurement period with no stimulation. The O_2Hb amplitude changes in the respective left hemisphere ROIs were much lower for the sham than real HD-tDCS session. Compared to the time course of O_2Hb in the stimulated left hemisphere ROIs, the non-stimulated right hemisphere ROIs (R_{in}, R_{out}) did not show differences between the sham and real-HD-tDCS session with O_2Hb amplitude staying close the baseline levels.

Figure 3 shows the group mean O_2Hb_{int} values of the left (stimulated) and right (non-stimulated) ROIs for the real (HD-tDCS-1, HD-tDCS-2) and sham sessions. The 2-way ANOVA revealed a significant main effect for Session ($F_{2,24}$=8.26, p=0.002) and ROI ($F_{3,36}$=78.57, p<0.001), as well as a Session x ROI interaction ($F_{6,72}$=10.88, p<0.001). Bonferroni corrected post-hoc tests showed that O_2Hb_{int} in the L_{in} ROI was significantly greater for the real HD-tDCS sessions (HD-tDCS-1: t(2)=6.9, p<0.01 and HD-tDCS-2: t(2)=7.0, p<0.01) compared to sham with no significant difference between HD-tDCS-1 and HD-tDCS-2. For both the real HD-tDCS sessions, L_{in} was significantly greater than L_{out} (HD-tDCS-1: t(2)=6.8, p<0.01 and HD-tDCS-2: t(2)=7.0, p<0.01), R_{in} (HD-tDCS-1: t(2)=11.5, p<0.01 and HD-tDCS-2: t(2)=11.2, p<0.01), and R_{out} (HD-tDCS-1: t(2)=11.1, p<0.01 and HD-tDCS-2: t(2)=10.7, p<0.01), and there was no significant difference between HD-tDCS-1 and HD-tDCS-2. For sham, there was no significant difference between L_{in} and L_{out}, but L_{in} was significantly greater than R_{in} (t(2)=3.3, p=0.008) and R_{out} t(2)=3.1, p=0.015). There were no significant differences between the real (HD-tDCS-1, HD-tDCS-2) and sham sessions for the right hemisphere ROIs (R_{in}, R_{out}).

The ICC calculated between the 2 real HD-tDCS sessions showed fair-to-good repeatability for left hemisphere ROIs (L_{in}: 0.54 and L_{out}: 0.52); while the ICCs from the right hemisphere ROIs indicated lower repeatability (R_{in}: 0.17 and R_{out}: 0.44).

Discussion

This is the first study to use multi-channel fNIRS to determine the spatial distribution of brain hemodynamics induced by anodal HD-tDCS using a 4x1 electrode montage. The main findings were that O_2Hb integral (O_2Hb_{int}) values of the fNIRS channels located within the spatial boundary of the 4x1 electrodes in the real HD-tDCS sessions (HD-tDCS-1 and HD-tDCS-2) in the left hemisphere ROIs (L_{in}) were significantly larger than the ROI located outside this

boundary (L_{out}) as well the non-stimulated right hemisphere ROIs (R_{in} and R_{out}). Since these focal hemodynamic effects were only seen in the two real HD-tDCS sessions, we consider that this differential distribution of O_2Hb_{int} between the L_{in} and L_{out} ROIs represents a hemodynamic correlate of the greater direct tissue effects of this 4x1 HD-tDCS montage electric field within the spatial extent of the 4x1 electrode montage, which confirm modeling (11) and neurophysiological (14) studies. Moreover, since the contralateral (unstimulated) right hemisphere ROIs (R_{in} and R_{out}) showed an overall decreased O_2Hb_{int} value for the sham and real HD-tDCS sessions, the greater O_2Hb_{int} findings in the left (stimulated) hemisphere provide an indirect indication for the spatial specificity of the anodal HD-tDCS electric field on the stimulated region of the left hemisphere. One added strength of the present study findings were that we included a second identical anodal HD-tDCS session to afford a within-subjects replication using ICCs, and the left hemisphere ROIs (L_{in} and L_{out}) showed fair-to-good repeatability.

It has been previously demonstrated that anodal tDCS-scalp applied electrical currents induce skin blood flow/erythema effects under the stimulating electrodes (36) through sensory axon reflex mechanisms (37). Since the strength of the electric field diminishes exponentially with distance from the electrode (24), the larger fNIRS O_2Hb_{int} values we found within the spatial extent of the 4x1 HD-tDCS electrodes (L_{in}) compared to outside (L_{out}) would suggest that there was a stronger electric field distribution in the L_{in} than L_{out} ROIs. From this argument, we can assume that connected network physiological effects were not the primary reason for the specific spatial distribution of O_2Hb_{int} within and outside the 4x1 HD-tDCS montage boundary of the stimulated left hemisphere. Using the reverse logic, if the specific spatial distribution of the fNIRS O_2Hb changes were due mainly to the direct 4x1 HD-tDCS electric field, then we can assume that this electric field was mainly concentrated within the boundaries of the 4x1 HD-tDCS electrode configuration as modeling studies predict (11, 14), and hence

has a greater chance of influencing the underlying cerebral tissue than regions outside this boundary.

Although there was a significantly greater O_2Hb_{int} for L_{in} vs L_{out} ROIs in the left stimulated hemisphere for the real HD-tDCS sessions compared to sham, the greater O_2Hb_{int} in the L_{out} ROI for real HD-tDCS compared to sham shows that the spatial focality is not so distinctive as reported by computational studies which show minimal current distributions outside the boundary of the 4x1 HD-tDCS montage (11). However, Edwards et al. (14) reported that 4x1 HD-tDCS montage using high voltage electrical currents evoke motor evoked potentials at locations both anterior and posterior to the M1 location although with a smaller amplitude, which indicates that current distributions of this 4x1 HD-tDCS montage can spread outside the 4x1 electrode boundary. Another reason for the spread of O_2Hb increases outside the boundary of the 4x1 HD-tDCS montage could be due to the specific way the fNIRS determine the spatial volume of O_2Hb concentrations. Since the locations of the fNIRS detector probes used for the channels of the L_{out} ROI were also the same ones used for the channels in the L_{in} ROI that were located at the boundary of the 4x1 electrodes (see Figure1), it is most likely that the primary cause for the greater O_2Hb_{int} values of the L_{out} ROI in the real HD-tDCS session compared to sham was the contribution of the increased hemodynamics at these boundary regions to the combined volume of tissue interrogated by the fNIRS light between the transmitters located further away.

It is important to indicate that the sham session also induced a numerically larger increase in O_2Hb_{int} values in the L_{in} compared to the L_{out} ROIs of the stimulated left hemisphere (see Figure 3), which were statistically larger compared to the right hemisphere ROIs (R_{in}, R_{out}). However, it should be noted that the sham session included active stimulation for 90s to mimic the sensations of the real HD-tDCS sessions. Therefore, in this active sham session we included a 30s ramp up from 0mA to 2mA current intensity, which was held for 30s at 2mA, and then

ramped down over 30s to 0mA, so there was 90s of active HD-tDCS applied to scalp during sham, which was sufficient to induce hemodymanic effects on the underlying tissues (See Figure 2a and figure 3). As shown in in Figure 2a for a representative subject's sham session, O_2Hb in L_{in} ROI increased from baseline over the 90s active stimulation period and soon after the stimulation was discontinued gradually returned to baseline levels over the remaining 510s measurement period. Since the O_2Hb changes returned to baseline after the stimulation was discontinued, while for the real HD-tDCS sessions the O_2Hb continued to increase and then plateau, we are confident that the O_2Hb changes in the stimulated left hemisphere ROIs (L_{in} and L_{out}) were due to the continued stimulation of the real HD-tDCS session, which the O_2Hb integral (O_2Hb_{int}) values appropriately classified as shown in the Figure 3. Nevertheless, the active sham session (active current applied for 1.5min duration) induces hemodynamic increases that are spatially bound to the 4x1 HD-tDCS montage and outlast the period of stimulation. These sham session findings corroborate with a recent study (36) that showed increased skin blood flow changes (erythema) within the boundaries of the scalp attached conventional ($25cm^2$) rubber/sponge electrodes after both real anodal tDCS (2mA for 30min duration) and active sham tDCS (2mA current applied for 1.5min duration), but the extent of the erythema with sham was significantly lower than the real anodal tDCS session.

Caveats and future directions

In our previous pilot study using a 2 channel time resolved fNIRS device (21) and modelling methods to disentangle scalp from cerebral hemodynamic changes (21, 34), we showed that during anodal HD-tDCS a greater portion of the fNIRS O_2Hb signals were derived from the scalp level skin blood flow changes in close proximity to the anode of the 4x1 electrode montage with a smaller proportion from the intracranial (cerebral) layer. In the present study, our findings of the grater spatial distribution of O_2Hb_{int} values within than outside the boundary

of the 4x1 electrodes (L_{in} > L_{out} ROI) were representing a direct tissue effect of the scalp applied HD-tDCS electric field stimulating scalp afferents and skin blood flow changes with a smaller proportion from the intracranial (cerebral) layer. These findings corroborate with experimental and theoretical data that approximately 50% of the total current applied to the scalp passes through to the cerebral layers and that the maximum current density is found in the cortices directly under the stimulating electrodes (24, 38). Future studies using time resolved fNIRS are necessary to disentangle the relative contribution of skin and cerebral hemodynamics during HD-tDCS.

Although our group level O_2Hb_{int} results showed a significant influence of the spatial distribution of anodal 4x1 HD-tDCS effects on the stimulated left hemisphere (L_{in} > L_{out}), at a single subject level there were differences in the time course of O_2Hb and corresponding O_2Hb_{int} values in the left stimulated hemisphere ROIs between the subjects. However, within-subjects the O_2Hb_{int} values in the L_{in} and L_{out} ROIs were moderately repeatable between the real HD-tDCS sessions (HD-tDCS-1 and HD-tDCS-2). These differences are most likely due to anatomical and physiological differences between subjects, which are known to be a contributor to variability in tDCS effects (7). Future studies are planned to determine the cause of the variability of the individual O_2Hb changes.

Overall, the present study findings provide a strong case that fNIRS neuroimaging can be used to determine an indirect hemodynamic measure of the spatial extent of the 4x1 HD-tDCS electric field in the stimulated hemisphere, which is reliable within subjects. The benefits of a neurophysiological (fNIRS) correlate of the HD-tDCS electric field compared to modelling its effects are that different HD-tDCS parameters and montages can be compared on the same subject and between subjects for their effects on a target cortical region, which allows for optimizing HD-tDCS parameters individually. This is based on the assumption that the spatial

distribution of the fNIRS O_2Hb changes overlying the target cortical region provides a surrogate marker of the spatial distribution of the scalp applied electric field.

In conclusion, our proof of concept study has provided evidence to confirm that fNIRS neuroimaging can be used to provide a hemodynamic correlate of the anodal 4x1 HD-tDCS electric field. We were able to show that anodal HD-tDCS with a 4x1 electrode montage can constrain the spatial distribution of O_2Hb_{int} to within the spatial extent of the 4x1 electrode configuration, which confirms modelling based predictions of the spatial distribution of the currents between electrodes. Future studies using different anodal HD-tDCS current intensities are necessary to determine the relationship between changes in O_2Hb_{int} and induced current density, such that it is envisaged that fNIRS will be able to inform of the HD-tDCS dosage that can be individually tailored to optimize HD-tDCS applications in natural settings to enhance motor and cognitive performance.

References

1. Parasuraman R, McKinley RA. Using noninvasive brain stimulation to accelerate learning and enhance human performance. *Hum Factors.* Aug 2014;56(5):816-824.

2. Jones KT, Stephens JA, Alam M, Bikson M, Berryhill ME. Longitudinal neurostimulation in older adults improves working memory. *PLoS One.* 2015;10(4):e0121904.

3. Nitsche MA, Paulus W. Excitability changes induced in the human motor cortex by weak transcranial direct current stimulation. *J Physiol.* 2000;527:633-639.

4. Muthalib M, Kan B, Nosaka K, Perrey S. Effects of transcranial direct current stimulation of the motor cortex on prefrontal cortex activation during a neuromuscular fatigue task: a fNIRS study. *Adv Exp Med Biol.* August 19-24 2013;789:73-79.

5. Stagg CJ, Nitsche MA. Physiological basis of transcranial direct current stimulation. *Neuroscientist.* Feb 2011;17(1):37-53.

6. Wiethoff S, Hamada M, Rothwell JC. Variability in response to transcranial direct current stimulation of the motor cortex. *Brain Stimul.* May-Jun 2014;7(3):468-475.

7. Li LM, Uehara K, Hanakawa T. The contribution of interindividual factors to variability of response in transcranial direct current stimulation studies. *Front Cell Neurosci.* 2015;9:181.

8. Berryhill ME, Peterson DJ, Jones KT, Stephens JA. Hits and misses: leveraging tDCS to advance cognitive research. *Front Psychol.* 2014;5:800.

9. Jacobson L, Koslowsky M, Lavidor M. tDCS polarity effects in motor and cognitive domains: a meta-analytical review. *Exp Brain Res.* Jan 2012;216(1):1-10.

10. Kessler SK, Minhas P, Woods AJ, Rosen A, Gorman C, Bikson M. Dosage considerations for transcranial direct current stimulation in children: a computational modeling study. *PLoS One.* 2013;8(9):e76112.

11. Datta A, Bansal V, Diaz J, Patel J, Reato D, Bikson M. Gyri-precise head model of transcranial direct current stimulation: improved spatial focality using a ring electrode versus conventional rectangular pad. *Brain Stimul.* Oct 2009;2(4):201-207, 207 e201.

12. Kuo HI, Bikson M, Datta A, et al. Comparing cortical plasticity induced by conventional and high-definition 4 x 1 ring tDCS: a neurophysiological study. *Brain Stimul.* Jul 2013;6(4):644-648.

13. Muthalib M, Besson P, Rothwell JC, Ward T, Perrey S. Effects of anodal high-definition transcranial direct current stimulation on bilateral sensorimotor cortex activation during sequential finger movements: an fNIRS study. *Adv Exp Med Biol.* 2016;876:351-359.

14. Edwards D, Cortes M, Datta A, Minhas P, Wassermann EM, Bikson M. Physiological and modeling evidence for focal transcranial electrical brain stimulation in humans: a basis for high-definition tDCS. *Neuroimage.* Jul 1 2013;74:266-275.

15. Stagg CJ, Lin RL, Mezue M, et al. Widespread modulation of cerebral perfusion induced during and after transcranial direct current stimulation applied to the left dorsolateral prefrontal cortex. *J Neurosci.* Jul 10 2013;33(28):11425-11431.

16. Zheng X, Alsop DC, Schlaug G. Effects of transcranial direct current stimulation (tDCS) on human regional cerebral blood flow. *Neuroimage.* Sep 01 2011;58(1):26-33.

17. Keeser D, Meindl T, Bor J, et al. Prefrontal transcranial direct current stimulation changes connectivity of resting-state networks during fMRI. *J Neurosci.* Oct 26 2011;31(43):15284-15293.

18. Cancelli A, Cottone C, Tecchio F, Truong DQ, Dmochowski J, Bikson M. A simple method for EEG guided transcranial electrical stimulation without models. *J Neural Eng.* Jun 2016;13(3):036022.

19. Roy A, Baxter B, He B. High-definition transcranial direct current stimulation induces both acute and persistent changes in broadband cortical synchronization: a simultaneous tDCS-EEG study. *IEEE Trans Biomed Eng.* Jul 2014;61(7):1967-1978.

20. Khan B, Hodics T, Hervey N, Kondraske G, Stowe AM, Alexandrakis G. Functional near-infrared spectroscopy maps cortical plasticity underlying altered motor

performance induced by transcranial direct current stimulation. *J Biomed Opt.* Nov 2015;18(11):116003.

21. Muthalib M, Re R, Besson P, et al. Transcranial direct current stimulation induced modulation of cortical haemodynamics: A comparison between time-domain and continuous-wave functional near-infrared spectroscopy. *Brain Stimul.* 2015;8:392.

22. Sood M, Besson P, Muthalib M, et al. NIRS-EEG joint imaging during transcranial direct current stimulation: Online parameter estimation with an autoregressive model. *J Neurosci Methods.* Sep 28 2016;274:71-80.

23. Amadi U, Ilie A, Johansen-Berg H, Stagg CJ. Polarity-specific effects of motor transcranial direct current stimulation on fMRI resting state networks. *Neuroimage.* Mar 2014;88:155-161.

24. Lang N, Siebner HR, Ward NS, et al. How does transcranial DC stimulation of the primary motor cortex alter regional neuronal activity in the human brain? *Eur J Neurosci.* Jul 2005;22(2):495-504.

25. Merzagora AC, Foffani G, Panyavin I, et al. Prefrontal hemodynamic changes produced by anodal direct current stimulation. *Neuroimage.* Feb 1 2011;49(3):2304-2310.

26. Attwell D, Iadecola C. The neural basis of functional brain imaging signals. *Trends in Neurosciences.* 12/1/ 2002;25(12):621-625.

27. Anwar AR, Muthalib M, Perrey S, et al. Effective Connectivity of Cortical Sensorimotor Networks During Finger Movement Tasks: A Simultaneous fNIRS, fMRI, EEG Study. *Brain Topogr.* Sep 2016;29(5):645-660.

28. Antal A, Bikson M, Datta A, et al. Imaging artifacts induced by electrical stimulation during conventional fMRI of the brain. *Neuroimage.* Oct 23 2013.

29. Turi Z, Paulus W, Antal A. Functional neuroimaging and transcranial electrical stimulation. *Clin EEG Neurosci.* Jul 2012;43(3):200-208.

30. Jones KT, Gozenman F, Berryhill ME. The strategy and motivational influences on the beneficial effect of neurostimulation: a tDCS and fNIRS study. *Neuroimage.* Jan 15 2015;105:238-247.

31. Yan J, Wei Y, Wang Y, Xu G, Li Z, Li X. Use of functional near-infrared spectroscopy to evaluate the effects of anodal transcranial direct current stimulation on brain connectivity in motor-related cortex. *J Biomed Opt.* Apr 2015;20(4):46007.

32. Ehlis AC, Haeussinger FB, Gastel A, Fallgatter AJ, Plewnia C. Task-dependent and polarity-specific effects of prefrontal transcranial direct current stimulation on cortical activation during word fluency. *Neuroimage.* Oct 15 2016;140:134-140.

33. Stephens JA, Berryhill ME. Older Adults Improve on Everyday Tasks after Working Memory Training and Neurostimulation. *Brain Stimul.* Jul-Aug 2016;9(4):553-559.

34. Muthalib M, Re R, Zucchelli L, et al. Effects of Increasing Neuromuscular Electrical Stimulation Current Intensity on Cortical Sensorimotor Network Activation: A Time Domain fNIRS Study. *PLoS One.* 2015;10(7):e0131951.

35. Basso Moro S, Bisconti S, Muthalib M, et al. A semi-immersive virtual reality incremental swing balance task activates prefrontal cortex: a functional near-infrared spectroscopy study. *Neuroimage.* Jan 15 2014;85 Pt 1:451-460.

36. Ezquerro F, Moffa AH, Bikson M, et al. The Influence of Skin Redness on Blinding in Transcranial Direct Current Stimulation Studies: A Crossover Trial. *Neuromodulation.* Oct 05 2016.

37. Durand S, Fromy B, Bouye P, Saumet JL, Abraham P. Vasodilatation in response to repeated anodal current application in the human skin relies on aspirin-sensitive mechanisms. *J Physiol.* Apr 01 2002;540(Pt 1):261-269.

38. Nitsche MA, Cohen LG, Wassermann EM, et al. Transcranial direct current stimulation: State of the art 2008. *Brain Stimul.* Jul 2008;1(3):206-223.

Figure Captions

Figure 1. Locations of the 16 fNIRS channels placed on the scalp of the left (Ch1-8) and right (Ch9-16) hemispheres (left panel). Each fNIRS channel was located midway between the transmitter (in yellow) and detector (in blue) probe. The anodal HD-tDCS 4x1 electrode montage are shown on the left hemisphere (anode electrode in red, 4 return electrodes in black). MNI coordinates (x,y,z) and Brodmann areas (BA) of the 16 fNIRS channels are reported on the right panel. In the stimulated left hemisphere, two regions of interest (ROIs) corresponded to the 4 channels within (L_{in}: Ch3,4,5,6 red shaded area) and outside (L_{out}: Ch1,2,7,8, blue shaded area) the spatial extent of the HD-tDCS 4x1 electrode montage, as well two ROIs in the corresponding channels on the right hemisphere (R_{in}: Ch11,12,13,14; R_{out}: Ch9,10,15,16).

Figure 2. Time course of oxygenated hemoglobin (O_2Hb) changes in a representative subject for the sham and real anodal HD-tDCS session determined from two regions of interest (ROIs) within (L_{in}) and outside (L_{out}) the spatial boundaries of the 4x1 electrode montage in the stimulated left hemisphere (panel a), as well as the two corresponding ROIs (R_{in}, R_{out}) in the right hemisphere (panel b). See Figure 1 for the fNIRS channels corresponding to the 4 ROIs.

Figure 3. Group mean (±SD) oxygenated hemoglobin integral (O_2Hb_{int}) values for the sham and two real (HD-tDCS-1, HD-tDCS-2) anodal HD-tDCS sessions determined from two regions of interest (ROIs) within (L_{in}) and outside (L_{out}) the spatial boundaries of the 4x1 electrode montage in the stimulated left hemisphere, as well as the two corresponding ROIs (R_{in}, R_{out}) in the right hemisphere. See Figure 1 for the fNIRS channels corresponding to the 4 ROIs. *: HD-tDCS-1 > sham, $p<0.001$; $^{+}$: HD-tDCS-2 > sham, $p<0.001$; $^{\#}$: HD-tDCS-1 L_{in} >

L_{out}, R_{in}, R_{out}, $p<0.001$; $^{\wedge}$: HD-tDCS-2 $L_{in} > L_{out}$, R_{in}, R_{out}, $p<0.001$; $^{\sim}$: sham $L_{in} > R_{in}$, R_{out}, $p<0.05$; $^{>}$: HD-tDCS-1 $L_{out} > R_{in}$, R_{out}, $p<0.01$; $^{<}$: HD-tDCS-2 $L_{out} > R_{in}$, R_{out}, $p<0.001$.

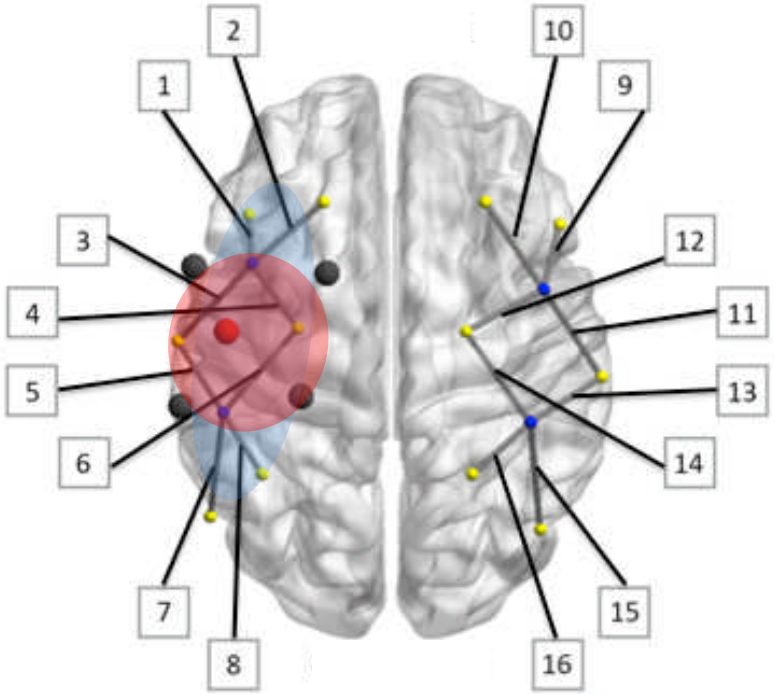

Channel	x	y	z	BA
1	-45	16	53	6-9-44
2	-37	18	60	6-8-9
3	-55	-6	53	3-4-6
4	-37	-4	65	4-6
5	-59	-31	52	1-2-3-40
6	-43	-27	68	1-3-4
7	-57	-52	50	39-40
8	-46	-49	60	2-7-39-40
9	51	13	50	6-9-44
10	42	15	59	6-8-9
11	59	-12	52	1-3-4-6
12	38	-6	67	4-6
13	55	-34	58	1-2-3-40
14	38	-26	72	3-4-6
15	48	-57	57	7-39-40
16	37	-53	69	1-2-7-40

a)

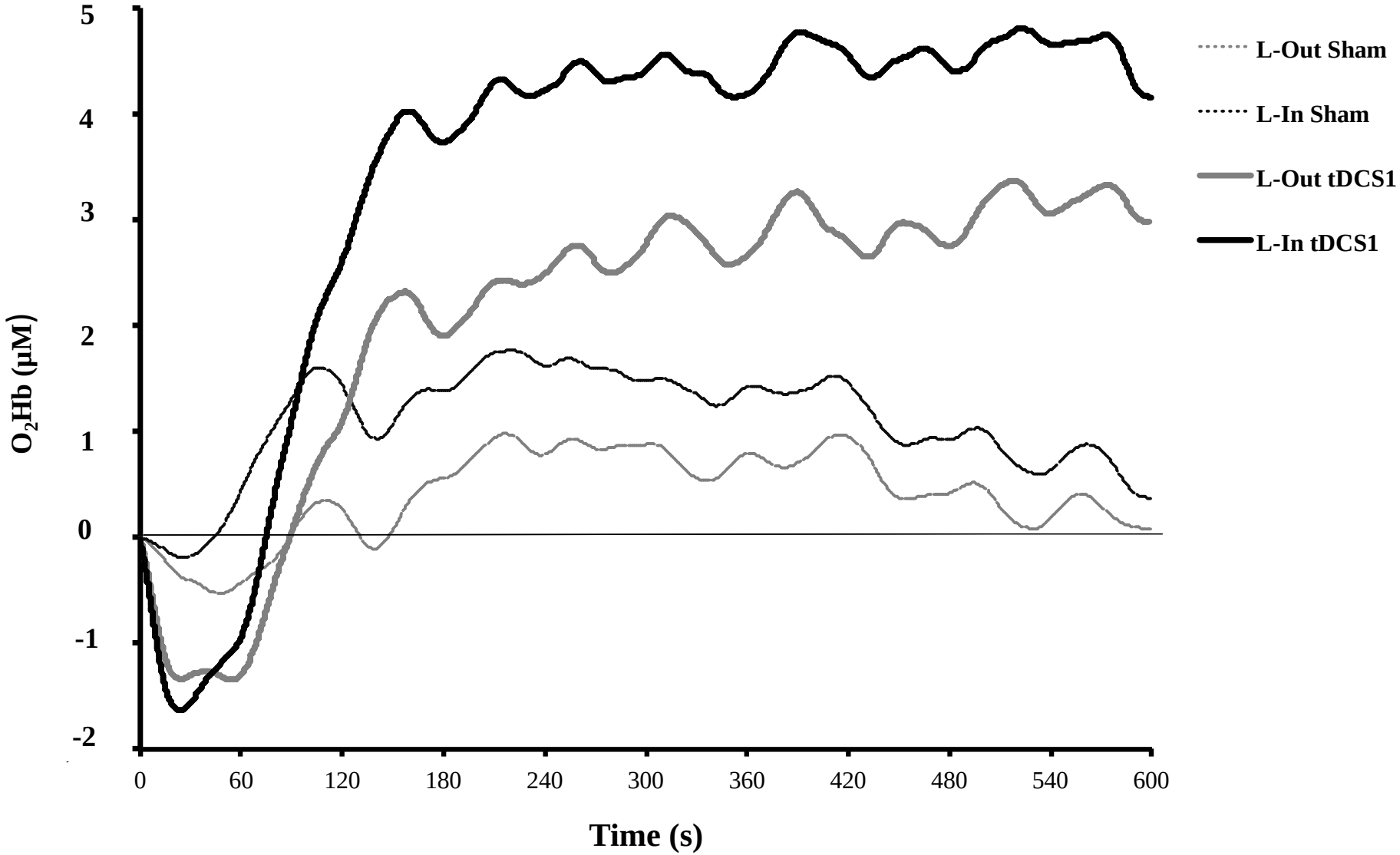
5
4
3
2
1
0
-1
-2
O2Hb (µM)
0
60
120
180
240
300
360
420
480
540
600
Time (s)
L-Out Sham
L-In Sham
L-Out tDCS1
L-In tDCS1

b)

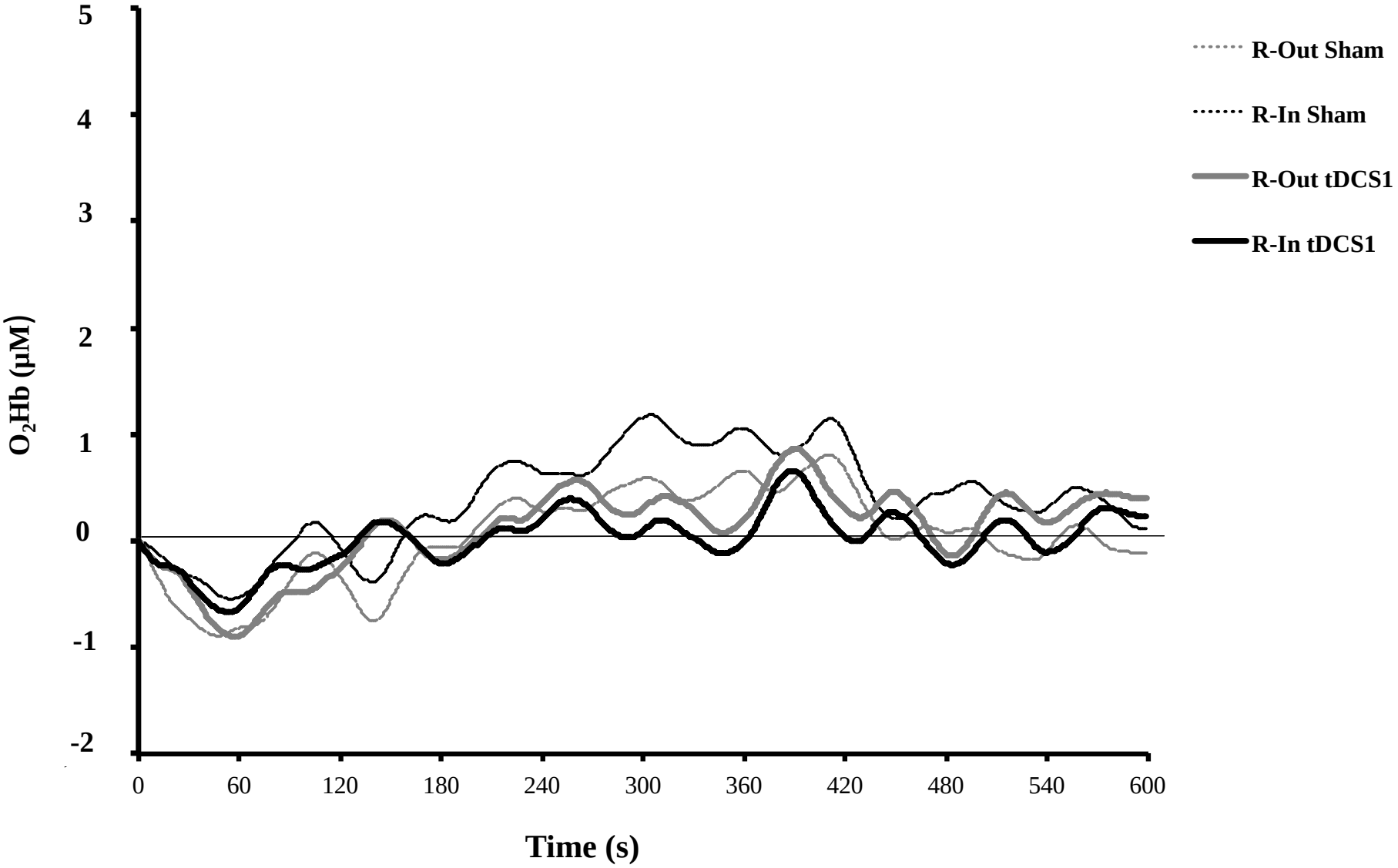
5
4
3
2
1
0
-1
-2
O2Hb (µM)
0
60
120
180
240
300
360
420
480
540
600
Time (s)
R-Out Sham
R-In Sham
R-Out tDCS1
R-In tDCS1

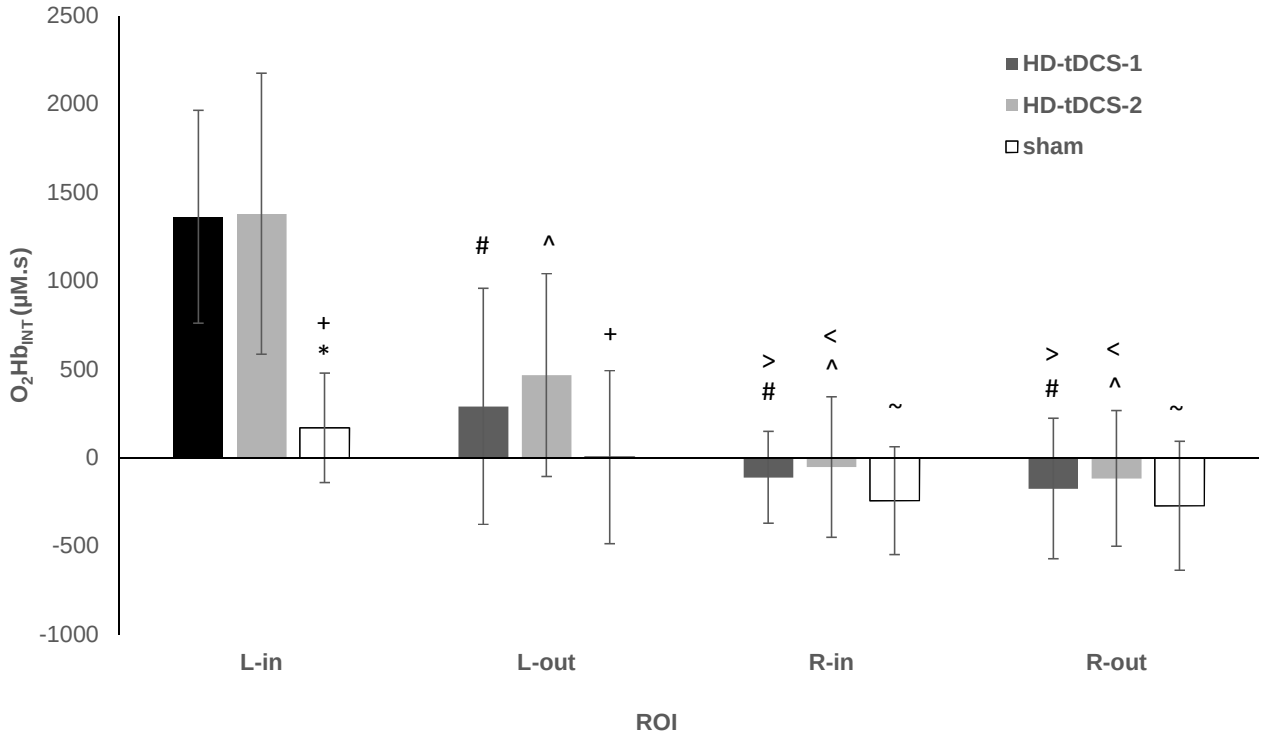
2500
2000
1500
1000
500
0
-500
-1000
O_2Hb_{INT} (µM.s)
HD-tDCS-1
HD-tDCS-2
sham
+
*
#
^
+
>
#
<
^
~
>
#
<
^
~
L-in
L-out
R-in
R-out
ROI

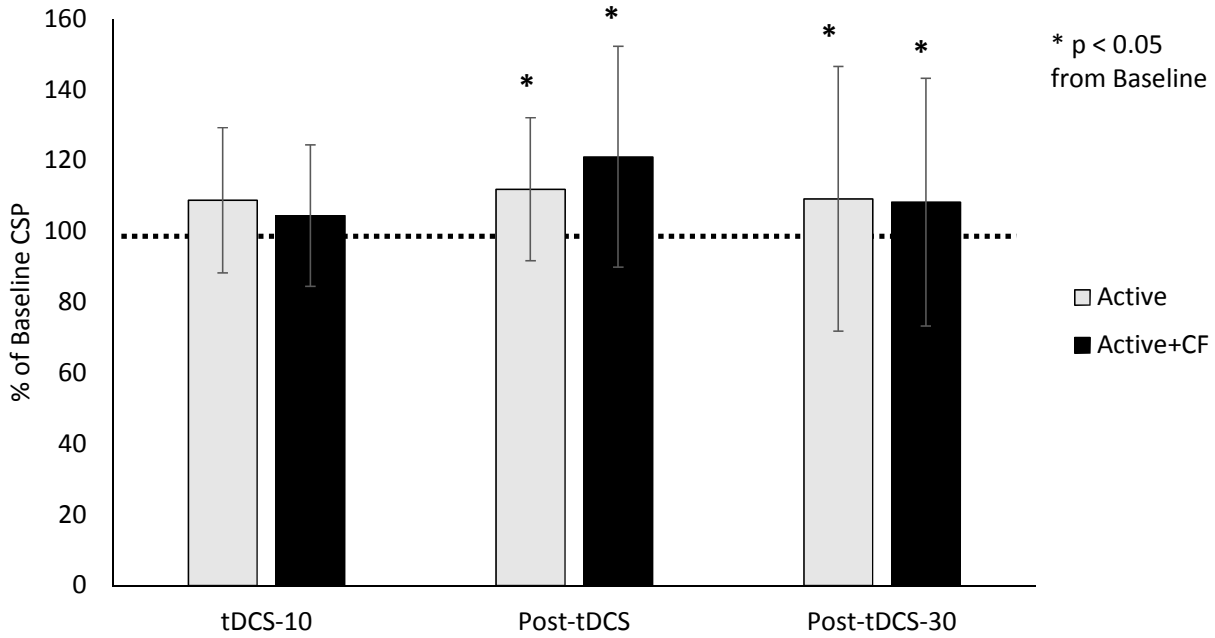
160
140
120
100
80
60
40
20
0
% of Baseline CSP
*
*
*
*
tDCS-10
Post-tDCS
Post-tDCS-30
* p < 0.05
from Baseline
Active
Active+CF